J. Fluid Mech. (1999), *vol.* 385, *pp.* 79–99. Printed in the United Kingdom

Insoluble surfactants on a drop in an extensional flow: a generalization of the stagnated surface limit to deforming interfaces

By CHARLES D. EGGLETON[1], YASHODHARA P. PAWAR[2] AND KATHLEEN J. STEBE[3]†

[1]Department of Mechanical Engineering, UMBC, Baltimore, MD 21250, USA

[2]Union Camp Corporation, Princeton, NJ 08543-3301, USA

[3]Department of Chemical Engineering, Johns Hopkins University, 3400 N. Charles Street, Baltimore, MD 21218, USA

(Received 23 July 1997 and in revised form 21 October 1998)

A drop in an axisymmetric extensional flow is studied using boundary integral methods to understand the effects of a monolayer-forming surfactant on a strongly deforming interface. Surfactants occupy area, so there is an upper bound to the surface concentration that can be adsorbed in a monolayer, Γ_∞. The surface tension is a highly nonlinear function of the surface concentration Γ because of this upper bound. As a result, the mechanical response of the system varies strongly with Γ for realistic material parameters. In this work, an insoluble surfactant is considered in the limit where the drop and external fluid viscosities are equal.

For $\Gamma \ll \Gamma_\infty$, surface convection sweeps surfactant toward the drop poles. When surface diffusion is negligible, once the stable drop shapes are attained, the interface can be divided into stagnant caps near the drop poles, where Γ is non-zero, and tangentially mobile regions near the drop equator, where the surface concentration is zero. This result is general for any axisymmetric fluid particle. For Γ near Γ_∞, the stresses resisting accumulation are large in order to prevent the local concentration from reaching the upper bound. As a result, the surface is highly stressed tangentially while Γ departs only slightly from a uniform distribution. For this case, Γ is never zero, so the tangential surface velocity is zero for the steady drop shape.

This observation that Γ dilutes nearly uniformly for high surface concentrations is used to derive a simplified form for the surface mass balance that applies in the limit of high surface concentration. The balance requires that the tangential flux should balance the local dilatation in order that the surface concentration profile will remain spatially uniform. Throughout the drop evolution, this equation yields results in agreement with the full solution for moderate deformations, and underscores the dominant mechanism at high deformation. The simplified balance reduces to the stagnant interface condition at steady state.

Drop deformations vary non-monotonically with concentration; for $\Gamma \ll \Gamma_\infty$, the reduction of the surface tension near the poles leads to higher deformations than the clean interface case. For Γ near Γ_∞, however, Γ dilutes nearly uniformly, resulting in higher mean surface tensions and smaller deformations. The drop contribution to the volume averaged stress tensor is also calculated and shown to vary non-monotonically with surface concentration.

† Author to whom correspondence should be addressed.

1. Introduction

The effect of surfactant adsorbed on a spherical droplet has been studied extensively in the limit where the surfactant is insoluble in the bulk fluid phase, and surface diffusion is negligible compared to surface convection. Under these conditions, a stagnant cap forms at the trailing pole. The formation of a stagnant cap on a spherical droplet settling at its terminal velocity has been addressed by Davis & Acrivos (1966), Sadhal & Johnson (1983), and He, Maldarelli & Dagan (1991) in the creeping-flow limit. As the sphere settles, surfactant adsorbed along the interface is swept toward the trailing pole, where it accumulates, creating a Marangoni stress that retards the surface flow. The surfactant mass balance in this limit demands that regions of non-zero surface concentration have zero tangential velocity. Thus, a stagnant cap forms where surfactant has accumulated. When the Marangoni stresses resisting surfactant accumulation are sufficiently pronounced, surfactant remains distributed along all of the drop interface, which is therefore rendered completely immobile.

In this paper, the problem of a drop in an extensional flow in the creeping-flow limit is used to extend our understanding of surfactant effects to strongly deforming interfaces. Insoluble monolayers are studied over a full range of surfactant concentration using a nonlinear model that accounts for monolayer saturation. Attention is limited to drops with the same viscosity as the external fluid phase. Stable drop shapes are shown to behave in a manner similar to the translating droplets; the interface becomes increasingly stagnated as the surface concentration is increased. During the deformation, however, the tangential surface flow is non-zero. A simple relationship is shown to exist between the normal and tangential velocities at high surface concentration as the drop shape evolves; it reduces to the no-slip condition at steady state.

When an initially spherical droplet is centred in a pure axisymmetric extensional flow, it deforms because of the viscous stresses exerted along the drop interface. This deformation is resisted by the surface tension. The ratio of the charateristic viscous stresses to surface tension is the capillary number, Ca. For a droplet in a quiescent system, surfactants adsorb to some surfactant concentration Γ_{eq}, reducing the surface tension to γ_{eq}. When fluid motion is imposed, the surfactant distribution is disturbed from this equilibrium, altering the stress conditions. In order to capture those effects not simply associated with the decrease in equilibrium tension, Ca is defined:

$$Ca = \frac{\mu G a}{\gamma_{eq}}, \tag{1}$$

where μ is the viscosity, G is the applied strain rate and a is the initial drop radius.

The droplet hydrodynamics are altered by surfactants through the interfacial stress balance (Levich 1962; Edwards, Brenner and Wasan 1991),

$$[[-p]]\boldsymbol{n} + [[\boldsymbol{n} \cdot \boldsymbol{T}]] = -\nabla_s \gamma + 2H\gamma \boldsymbol{n}, \tag{2}$$

where p is the isotropic pressure, $\boldsymbol{T}$ is the viscous stress tensor, the brackets indicate the jump between internal and external phases, γ is the surface tension, $\boldsymbol{n}$ is the surface normal, ∇_s is the surface gradient operator, and $2H$ is the mean curvature of the interface. The Marangoni stress $\nabla_s \gamma$ is exerted tangentially; the Laplace pressure $2H\gamma$ acts normally.

These interfacial stresses are coupled with the surface velocity and the surface mass balance. The tangential streamlines on a surfactant-free droplet centred in an extensional flow are indicated by the arrows along the drop interface in figure 1.

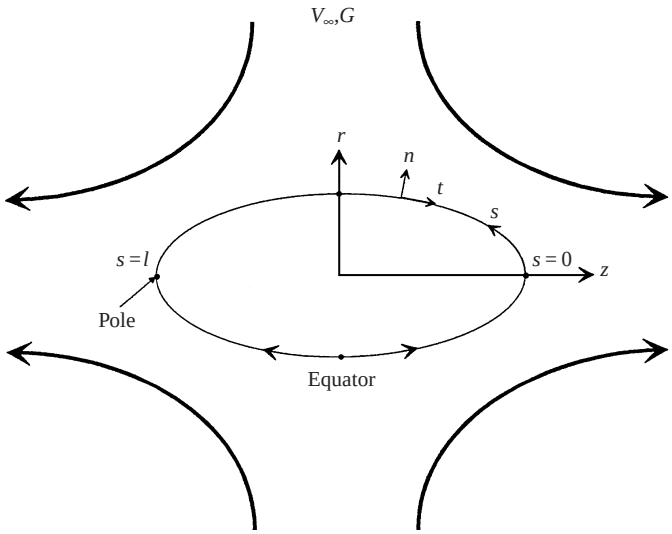

FIGURE 1. A neutrally buoyant drop is suspended in an immiscible fluid of equal viscosity and subjected to a pure axisymmetric extensional flow. The position of the interface is described by a cylindrical coordinate system (r, z). An arclength parameterization is adopted, $r = r(s)$ and $z = z(s)$, s being the arclength parameter, $0 < s < l$ from drop pole to pole.

There is a ring at the drop equator and poles at the drop tips where the tangential surface velocity v_t is zero. The surface flow diverges from the ring, and flows toward the drop tips. Adsorbed surfactant is convected from the equator and toward the drop tips creating surface tension gradients that alter the stresses and therefore the surface velocity.

Previous work on this problem is reviewed by Stone & Leal (1990), who first considered the coupling between surfactant effects and drop deformation for leading-order deformations. Only the more recent contributions are discussed here. In the limit of dilute surface concentrations, Stone & Leal, and Milliken, Stone & Leal (1993) studied the effect of insoluble surfactants on the drop deformation. Milliken & Leal (1994) extended this work to include surfactant solubility and non-unity viscosity ratios. All of these studies either used a linear surface equation of state to relate the surface tension and the surface concentration of adsorbed surfactant, or were limited to concentrations that were sufficiently dilute that the linear approximation was valid. At higher concentrations, surface saturation and non-ideal surfactant interactions influence the stresses realized. Pawar & Stebe (1996) studied the effects of surfactant interactions. Cohesive interactions strong enough to induce surface phase changes were also studied.

In this paper, the deforming-drop problem is re-investigated to understand how the mechanical response of the interface varies with surfactant concentration for a nonlinear surface tension model which accounts for the finite dimensions of surfactant molecules. Because surfactant molecules have finite dimensions, there is an upper bound to the surface concentration, Γ_∞, that can be accommodated in a monolayer. This is reflected in the surface equation of state shown as a graph in figure 2, in which the surface tension reduction caused by surfactant adsorption (the surface pressure $\Pi = \gamma_0 - \gamma$, where γ_0 is the surface tension of the surfactant-free interface) is shown as a function of the normalized area per surfactant molecule at the interface, Γ_∞/Γ, where Γ is the surface concentration of surfactant in the monolayer. This is a graph

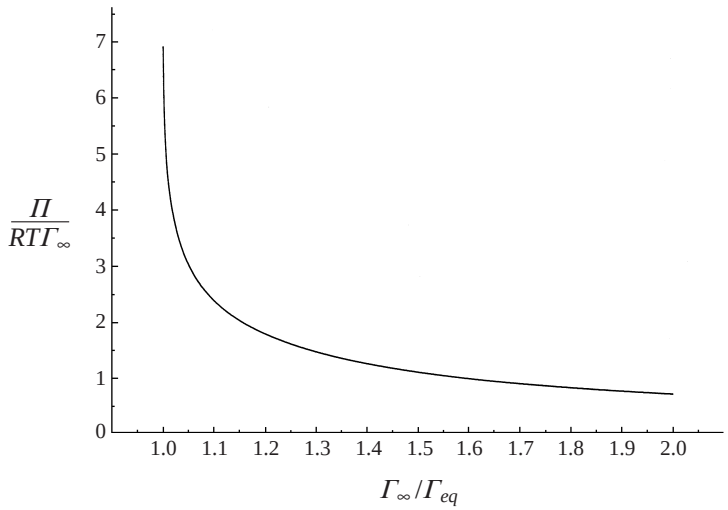

FIGURE 2. Surface pressure Π *vs.* normalized area per molecule Γ_∞/Γ for the Von Szyckowski model. As the minimum area/molecule is approached, the surface pressure diverges.

of the Von Szyckowski equation:

$$\frac{\Pi}{RT\Gamma_\infty} = \frac{\gamma_o - \gamma}{RT\Gamma_\infty} = -\ln\left(1 - \frac{\Gamma}{\Gamma_\infty}\right), \tag{3}$$

where the surface pressure Π is the work per unit area which must be done to compress the monolayer. This equation of state can be derived from a regular solution theory for a monolayer (Guggenheim 1952; Defay & Prigogine 1966) or from an adsorption-kinetic approach (Frumkin 1925). (In (3), the terms accounting for surfactant interaction have been neglected.)

In (3), as Γ approaches Γ_∞ (i.e. as the surfactant area/molecule approaches its minimum) the work required to compress the surface diverges logarithmically because of the area excluded by the finite surfactant cross-section. The derivative of the surface tension with respect to Γ is:

$$\frac{\partial\gamma}{\partial\Gamma} = -\frac{RT}{(1 - \Gamma/\Gamma_\infty)}. \tag{4}$$

As Γ approaches Γ_∞, (4) diverges as a first-order pole. The Marangoni stresses, which can be expressed as:

$$-\nabla_s\gamma = -\frac{\partial\gamma}{\partial\Gamma}\nabla_s\Gamma \tag{5}$$

are therefore proportional to (4). For physically realizable Γ values (for which the surface tension is finite), strong changes in the mechanical properties of the system as the pole is approached prevent it from being reached. This is similar to any simple thermodynamic model that accounts for space-filling molecules (e.g. square-well or Lennard–Jones potentials).

Typically, $RT\Gamma_\infty \ll \gamma_0$, so the surface tension does not reduce appreciably unless Γ is near Γ_∞. Therefore, for systems with trace surface active impurities, $\Gamma_{eq} \ll \Gamma_\infty$ and $\gamma_{eq} \approx \gamma_0$. For systems to which surfactants have been deliberately added to reduce the surface tension, however, Γ_{eq} must approach Γ_∞. The highly nonlinear response of

the Marangoni stress in this concentration regime regulates the surface concentration so that the minimum area/molecule is not reached and the surface tension remains finite. This nonlinear response strongly alters the hydrodynamics.

In this work, the stagnant cap limit is shown to apply to deformed, axisymmetric droplets once a stable drop shape is attained. The area occupied by the stagnant cap depends on the amount of surfactant adsorbed. If the surface concentration is very low (i.e. the initial surface concentration $\Gamma_{\mathrm{eq}} \ll \Gamma_{\infty}$), small Marangoni stresses develop as the flow creates gradients in the surface concentration. This allows the surfactant to be collected at the drop poles, creating immobile cap regions and mobile regions near the equator. Because of the local reduction in the surface tension near the pole, larger deformations result than the clean case.

At elevated surface concentration (i.e. with Γ_{eq} only slightly less that Γ_{∞}) only weak surface concentration gradients form. When the flow is initiated, the tangential velocity v_t tends to sweep surfactant toward the poles. However, because of the singularity in (4), the Marangoni stress is elevated even for small gradients in Γ, significantly slowing v_t. As a result, Γ is forced to remain nearly uniform, but the surface is highly stressed tangentially. The mean surface tension increases with surface dilatation, so smaller deformations result. The droplet deformation cannot be described by simply accounting for the pure dilution in the Laplace pressure. Rather, the manner in which the Marangoni stresses have altered the surface tension must be taken into account in order to describe the system in this limit.

These observations are used to propose a modified surface mass balance for the high coverage limit which relates the global dilatation of the interface to the local dilatation. The balance requires that the tangential flow should balance local surface dilatation so as to maintain a uniform surface concentration. The mass balance is a generalization to deforming interfaces of the stagnant interface limit commonly encountered in the study of surfactant-laden non-deforming interfaces. Indeed, once the steady deformation is attained, the surface velocity does reduce to zero.

The particle contribution to the volume average stress tensor for this flow is calculated. The axial component varies monotonically with the surface concentration, as do the Marangoni stresses. However, the radial component varies non-monotonically with Γ_{eq} and is dominated by changes in cross-sectional area except at the highest surface concentrations studied, where the pronounced Marangoni stresses dominate.

2. Governing equations

2.1. *Hydrodynamics*

An initially spherical droplet is centred in a pure axisymmetric extensional flow at a strain rate G. Both the droplet and outer fluids have viscosity μ. The subscript 1 (2) denotes the outer (droplet) fluid. The velocity and pressure fields in the drop and external phases are denoted by $\boldsymbol{v}_i$ and p_i, with $i = 1, 2$, respectively. The position vector defined with respect to the centre of mass of the drop is denoted by $\boldsymbol{r}$. Initially, the droplet radius is a and the surface concentration is Γ_{eq}. Corresponding to this surface concentration is an initial surface tension γ_{eq}. The governing equations are cast in dimensionless form according to the following scales:

$$\boldsymbol{v}_i^* = \frac{\boldsymbol{v}_i}{Ga}; \quad p_i^* = \frac{p_i a}{\gamma_{eq}}; \quad \boldsymbol{T}^* = \frac{\boldsymbol{T}}{\mu G}; \quad t^* = tG; \quad \gamma^* = \frac{\gamma}{\gamma_{eq}}; \quad \Gamma^* = \frac{\Gamma}{\Gamma_{eq}}; \quad \boldsymbol{r}^* = \frac{\boldsymbol{r}}{a}, \tag{6}$$

where dimensionless variables are noted with *. Adopting a local state assumption, γ^* is determined by the local Γ^* according to the surface equation of state (3), recast

in dimensionless form as:

$$\gamma^* = \frac{\gamma_0}{\gamma_{eq}} + E\ln(1 - x\Gamma^*). \tag{7}$$

In this equation, two dimensionless quantities appear, the elasticity number E, a measure of the sensitivity of the surface tension to Γ:

$$E = \frac{RT\Gamma_\infty}{\gamma_{eq}}, \tag{8}$$

and the fraction of the interfacial area that is initially covered by surfactant, x.

$$x = \frac{\Gamma_{eq}}{\Gamma_\infty}. \tag{9}$$

Fixing E and x determines γ_{eq}/γ_o:

$$\frac{\gamma_{eq}}{\gamma_o} = \frac{1}{1 - E\ln(1 - x)}. \tag{10}$$

Typical parameter values for E and x are discussed below.

For the remainder of the paper, only dimensionless variables are used unless explicitly noted; the superscript * is dropped for conciseness. The flow in the droplet and external phases is governed by the incompressible Stokes equations:

$$\nabla^2 \boldsymbol{v}_i = \nabla p_i; \quad \nabla \cdot \boldsymbol{v}_i = 0, \tag{11}$$

where $i = 1,\ 2$, respectively.

The velocity of the outer fluid, $\boldsymbol{v}_1$, must agree with the imposed axisymmetric extensional velocity far from the droplet:

$$\lim_{x\to\infty} \boldsymbol{v}_1 = \boldsymbol{v}_\infty = \begin{bmatrix} -1 & 0 & 0 \\ 0 & -1 & 0 \\ 0 & 0 & 2 \end{bmatrix} \cdot \boldsymbol{r}. \tag{12}$$

At the interface, the velocities are continuous:

$$\boldsymbol{v}_1 = \boldsymbol{v}_2 = \boldsymbol{v}_s. \tag{13}$$

In this expression, $\boldsymbol{v}_s$ is the surface velocity, which can be expressed in terms of normal ($\boldsymbol{v}_n$) and tangential ($\boldsymbol{v}_t$) components.

The kinematic condition at the interface requires:

$$\frac{\mathrm{d}\boldsymbol{r}_s}{\mathrm{d}t} = \boldsymbol{v}_n, \tag{14}$$

where $\boldsymbol{r}_s$ is the position vector of a Lagrangian point on the interface. The stress balance, given in (2), is recast in dimensionless form:

$$[[-p]]\boldsymbol{n} + Ca[[\boldsymbol{n} \cdot \boldsymbol{T}]] = -\frac{E}{1 - x\Gamma}\nabla_s\Gamma + 2H\gamma\boldsymbol{n}. \tag{15}$$

The dimensionless surface mass balance takes the form:

$$\frac{\partial\Gamma}{\partial t} + \nabla_s \cdot (\Gamma \boldsymbol{v}_t) - \frac{1}{Pe_s}\nabla_s^2\Gamma + 2H\Gamma\boldsymbol{v}_n = 0, \tag{16}$$

where the time derivative is defined for displacements of the surface coordinates normal to the interface as assumed implicitly by Stone (1990) and discussed in detail

by Wong, Rumschitzski & Maldarelli (1996). This balance contains the surface Péclet number, Pe_s, defined as:

$$Pe_s = Ca\Lambda, \tag{17}$$

where

$$\Lambda = \frac{\gamma_{eq} a}{\mu D_s} \tag{18}$$

depends only on material constants. By fixing the surfactant material parameters and initial coverage, (E, Λ, and x), the response of the drop with fixed surfactant properties to increasing strain rates can be followed by increasing Ca.

The governing equations are recast in an arc-angle formulation where the arclength s varies from 0 to l, l being a dimensionless contour length measured from one drop 'tip' to the other. The contour length l increases from its initial value of π as the drop elongates. The interface location, $r(z)$, is parameterized in arclength, i.e. $r(s)$ and $z(s) = 0$. The drop equator is located at the arclength for which $z(s) = 0$; the drop tips are located at $r(0) = r(l) = 0$. This parameterization obeys:

$$\left(\frac{\partial r}{\partial s}\right)^2 + \left(\frac{\partial z}{\partial s}\right)^2 = 1. \tag{19}$$

In terms of arc-angle coordinates, the surface mass balance becomes:

$$\frac{\partial \Gamma}{\partial t} + \frac{\partial}{\partial s}(r v_t \Gamma) + 2H v_n \Gamma - \frac{1}{\Lambda Ca\, r}\frac{\partial}{\partial s}\left[r\frac{\partial \Gamma}{\partial s}\right] = 0. \tag{20}$$

Stokes' equations are recast in terms of boundary integral equations to give $\boldsymbol{v}_s$ for a droplet in an axisymmetric flow field for fluids of equal viscosity. (Ladyzhenskaya 1969):

$$\boldsymbol{v}_s(\boldsymbol{x}_s) = \boldsymbol{v}_\infty(\boldsymbol{x}_s) - \frac{1}{8\pi}\int_{s=0}^{s=1} \boldsymbol{M}(\boldsymbol{x}_s, \zeta) \cdot \left[\left[-\frac{p}{Ca}\boldsymbol{n} + \boldsymbol{n}\cdot\boldsymbol{T}\right]\right](\zeta)\, \mathrm{d}s(\zeta), \tag{21}$$

where $\boldsymbol{M}$ is the axisymmetric Green's function for Stokes' flow and ζ is an integration variable along the interface. Singular behaviour in the normal stress is avoided by a technique discussed in Pozrikidis (1992), i.e. the property that $\boldsymbol{M}$ obeys the incompressible equation of continuity is used to subtract away the diverging terms in the neighbourhood of the pole. The singularity in the tangential stress is avoided in a similar manner.

These equations are used to find the drop deformation, surface tension and concentration profiles that occur as a function of Ca. Here, they are integrated as a function of surface coverage x to understand the effect of surface concentration on the interfacial mechanics. In the limit of nearly saturated monolayers, they are used to guide a reformulation of the mass balance. The details of the solution technique are given in Pawar & Stebe (1996). The implementation was modified slightly in order to obtain stable results at the high surface coverages considered.

2.2. *Parameter values*

In all previous surfactant-related work in this flow, the elasticity number E (or the corresponding parameter for a linear adsorption isotherm) has been taken to be order one. While this allows the interplay of Marangoni stresses and deformation to be elucidated, these values are far larger than those typically realized physically, and prevent the low-concentration regime from being properly understood by overestimating the strength of the coupling between concentration and surface tension.

Surfactant		$RT\Gamma_\infty$ (mN/m)	γ_{CMC} (mN/m)	E_{min}	E_{max}	X_{CMC}
$C_{12}E_8$	(a/w)	5.06	34	0.07	0.15	0.999
$C_{12}E_6$	(a/w)	5.99	32	0.08	0.19	0.998
TritonX 100	(a/w)	7.22	30	0.10	0.24	0.997
	(o/w)	4.86	9.2	0.08	0.53	> 0.999
DPPC*	(a/w)	10	30	0.15	0.31	–

The notation (a/w) indicates air/aqueous interfaces; (o/w) indicates oil/aqueous interfaces. These data were drawn from the following sources. The polyethoxylated surfactant $C_{12}E_8$ was studied by Lin *et al* (1996); $C_{12}E_6$ was studied by Pan, Green & Maldarelli (1998), where the notation C_nE_m denotes the structure $H_3C\text{-}(CH_2)_{m-1}\text{-}(OCH_2CH_2)_n\text{-}OH$. The Triton-X 100 data appears in Stebe *et al.* (1989), where Triton-X 100 is the commercial name for the surfactant with the structure $CH_3C(CH_3)_2\text{-}CH_2C(CH_3)_2C_6H_4\text{-}(OCH_2CH_2)_n\text{-}OH$, n between 9 and 10.

*DPPC denotes dipalmitoyl phosphatidyl choline, a lipid that forms insoluble monolayers at aqueous–air interfaces. Γ_∞ is the inverse minimum area per molecule to which these monolayers can be compressed, 41 A^2/molecule. This molecule does not form micelles. The maximum surface pressure to which this monolayer can be slowly compressed is about 40 dyn cm^{-1}, or a surface tension of 32 dyn cm^{-1}. This is reported for the minimum $\gamma(\gamma_{cmc})$ column.

TABLE 1. Material parameters for the calculation of the elasticity number.

In table 1, parameter ranges for E and x are calculated based on data for a number of surfactants at aqueous–air and aqueous–oil interfaces. (Material constants for a wide variety of soluble surfactants which are adequately described by (3) are also provided in the recent review of Chang & Franses (1995).)

The numerator of E is independent of concentration. The denominator can be, at most, the value at the surfactant-free interface, γ_o, and, for soluble surfactants, at least γ_{CMC}, the value at a concentration termed the critical micelle concentration, or CMC. (At this concentration, surfactants form aggregates, termed micelles, in the bulk. For concentrations greater than the CMC, the monomer concentration remains roughly at the CMC with additional surfactant forming micelles. The surface tension does not diminish with bulk concentration above this concentration.) Defining E in terms of these two tensions provides a minimum and maximum value for this parameter for a particular surfactant. For strictly insoluble amphiphiles, surface pressure isotherms can be complicated, with features such as phase transitions that cannot be described simply by (3). (The hydrodynamic implications of these features are discussed in Pawar & Stebe.) However, the surface saturation aspects of these monolayers are adequately described by this expression. In this work, the value for E is set to 0.2, which falls within the range of values reported in table 1.

The surface coverages x considered in this paper vary from the extremely dilute ($x = 0.01$) to extremely concentrated ($x = 0.996$). In practice, x can assume these values. Supporting data are presented in table 1. For the soluble molecules, x at the CMC is always greater than 0.99. For insoluble surfactants on a Langmuir trough, x can also be forced to such values. Thus, the parameter values considered here (x ranging from 0.01 to 0.996 and E of 0.2) are physically relevant.

The linear model adopted in prior studies can be derived from (7) in the limit of $x \ll 1$,

$$\gamma = 1 - Ex\Gamma. \tag{22}$$

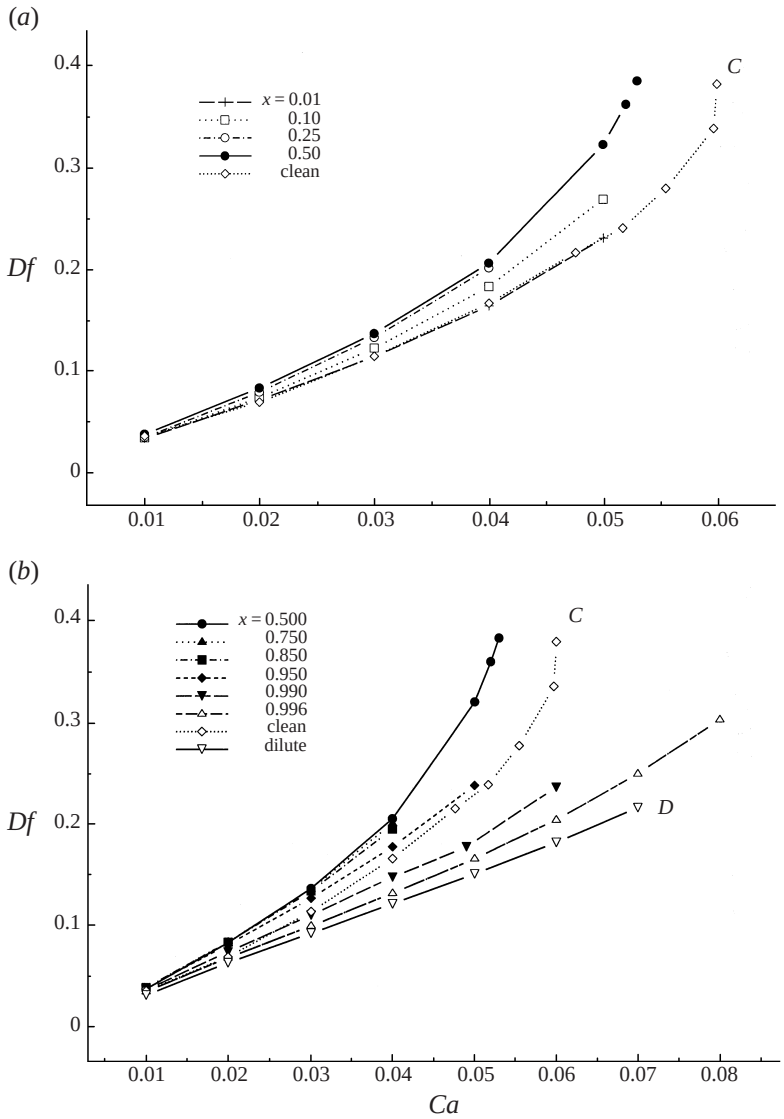

FIGURE 3. Deformation Df *vs.* Ca for (*a*) $0.01 \leqslant x \leqslant 0.5$ and (*b*) $0.5 \leqslant x \leqslant 0.996$. Curve C is the clean interface result; curve D is the pure dilution $x = 0.996$ result.

Using the parameters in table 1, the magnitude of Ex is roughly 0.02 for an aqueous–air surfactant system with a dilute surface coverage x of 0.1. However, the slope of the surface tension has been taken to be much larger (e.g. Ex in excess of 0.8 was adopted in Stone & Leal 1990).

Typically, surface diffusion is extremely weak. In this study, Λ is held fixed at $1000\gamma_o/\gamma_{eq}$. This value for Λ is actually an underestimate for a typical surfactant. Surface diffusivities are of the order of 10^{-6} cm^2 s^{-1}, viscosities are of the order of 1 cp; for drops of initial radius of 1 cm, this group is about 10^7.

3. Results and discussion

The drop deformation, Df is shown in figure 3. (Df is presented in terms of the difference between the length and breadth of the drop over the sum of these quantities; Df of 0.33 is a 2:1 ellipsoid). First, consider the curve marked C. This corresponds to the clean droplet deformation result of Blundell & Duffy (as reported in Rallison 1984). For this case, the surface tension is uniform, and no Marangoni stresses are exerted along the interface. This limit can be attained for two cases: either a surfactant-free drop, or a surfactant for which mass transfer by exchange with the bulk is sufficiently rapid that Γ is unity everywhere on the interface. (This rapid mass transfer limit was confirmed in the results of Milliken & Leal (1994) for soluble surfactants and linear surface equations of state and by Eggleton & Stebe (1998) for the nonlinear equation of state adopted in this study.)

Deformations that fall above the C curve occur when the dominant mechanism is tip stretching, i.e. surface convection causes surfactant to accumulate at the drop tips, locally reducing the surface tension. In order to balance the normal stress jump, the local curvature increases, causing the drop to elongate. For deformations that fall beneath the C curve, interfacial dilution is the dominant mechanism. Surfactant remains uniformly distributed over the stretching interface. The mean surface tension therefore increases, resisting stretching more strongly than the equilibrium tension, and smaller deformations result. In Stone & Leal (1990), the tip stretching regime was realized for weak coupling between the surface tension and the surface concentration and weak surface diffusion (high Λ). Uniform coverages were realized for strong surface diffusion or strong coupling between the surface concentration and the tension.

Here, the full range of deformations is realized as a function of surface coverage x for fixed, realistic surfactant material parameters. Drop deformations for $x \leqslant 0.5$ are presented in figure 3(a). The deformations for $x = 0.01$ superpose with the clean interface result, agreeing to within 0.01%. For x greater than or equal to 0.1, all drop deformations are greater than the surfactant-free drop, and Df increases monotonically with x. Tip stretching is dominant. For $0.996 \geqslant x \geqslant 0.5$, drop deformations are reported in figure 3(b). Over this range of x, deformations decrease monotonically with x; for x of 0.996, the deformations fall strongly in the dilution dominated regime for all Ca studied.

Consider first the $x \leqslant 0.5$ results. (For all profiles presented as a function of arclength, the arclength s is normalized by the drop half-length l. This allows the comparison of profiles realized on drops of different lengths on a single graph.) Gradients in Γ decrease with x. The product $x\Gamma$ (or Γ/Γ_∞ in dimensional form) is shown in figure 4(a), the Marangoni stresses are presented in figure 4(b). The greater x values have higher local surface concentrations and stronger Marangoni stresses in the region of the tip. This strongly reduces the local surface tensions (see the surface tensions in figure 4c), increasing tip stretching.

Consider the surface concentration and Marangoni stress profiles for $x = 0.1$ shown in figures 4(a) and 4(b). The surface concentration has pronounced accumulation in the tip region, and falls nearly to zero near the equator. The Marangoni stresses are highly skewed toward the drop tip, and also fall to zero near the equator. These profiles correspond to stagnant cap behaviour. The strong accumulation of surfactant near the drop tips occurs because of the initially weak Marangoni stresses (which are roughly equal to $Ex\nabla_s\Gamma \cong 0.02\nabla_s\Gamma$). When the extensional flow is initiated, these stresses are too weak to oppose the formation of Γ gradients. Surfactant accumulates strongly at the poles; regions near the equator are swept clean of surfactant. The accumulation causes strong local Marangoni stresses to develop near the tips. For

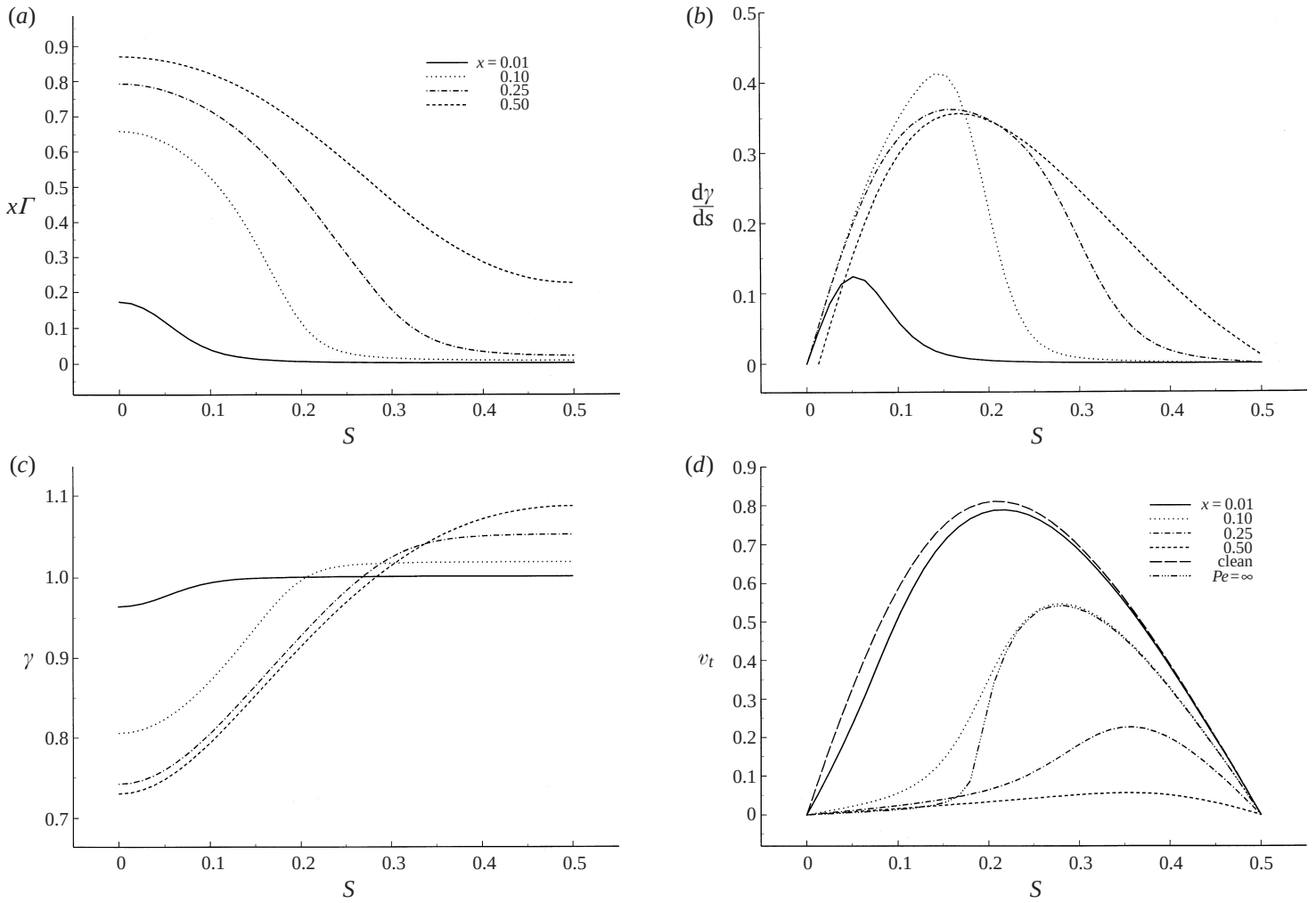

FIGURE 4. Families of curves as a function of x for $x \leqslant 0.5$ for $Ca = 0.04$. The legend for all of figure 4 is an inset to figure 4(*a*). (*a*) $x\Gamma$ *vs. s* profiles. (*b*) Marangoni stress *vs. s* profiles. (*c*) γ *vs. s* profiles. (*d*) v_t *vs. s* profiles.

dilute x at fixed Ca, then, the interface has surfactant-rich and surfactant-free regions at steady state. Such a steady profile was also realized in the study of Stone & Leal (1990) for the large surface Péclet number and for weak coupling between the surface tension and the surface concentration. (See figure 3, the $\beta = 0.1$ graph on p. 180 of Stone & Leal.) The significance of this profile in terms of stagnant cap formation was not noted, however.

Stagnant caps must form once stable drop shapes have been attained when the surface diffusion is negligible. Requiring v_t and $r(s)$ to be zero at the poles, the mass balance (20) becomes:

$$\Gamma v_t = 0. \tag{23}$$

That is, on the interface of any steady axisymmetric particle, the tangential velocity or the surface concentration is zero for insoluble surfactants with negligible surface diffusion.

The tangential velocity profile for the droplet that has attained its steady shape (to within our convergence criterion, for which $v_n < 5\times10^{-4}/Ca$) is shown in figure 4(d). For $x = 0.1$, v_t is nearly zero at the tip, whereas surfactant-free regions of the interface have strong tangential flow. For the higher surface coverages studied, the surface concentration is not zero anywhere on the drop interface, and so the steady tangential velocities are strongly reduced everywhere. These results are for large, finite Λ. The resulting weak surface diffusion flux balances the weak convective flux of surfactant at steady state, allowing non-zero velocities in the surfactant-covered regions. When Λ is infinite, v_t is strictly zero near the drop tips, as shown for $x = 0.1$ in figure 4(d). The area stagnated increases with x; for $x = 0.5$, the entire interface is stagnated.

Consider now the results for $0.996 \geqslant x \geqslant 0.5$. The corresponding surface concentration, Marangoni stress and surface tension profiles are given in figure 5(a)–5(d), respectively. The Γ profiles for x approaching unity are nearly spatially uniform. For example, for $x = 0.996$, the initial Marangoni stresses are roughly $Ex\nabla_s\Gamma/(1-x) \approx 50\nabla_s\Gamma$; tangential stresses are large even for perturbative gradients in Γ. The result is an interface that is highly stressed tangentially, reducing the surface convective flux of surfactant toward the drop poles, and forcing $x\Gamma$ to remain locally less than 1. In this manner, the limiting area/molecule is enforced by the tangential stress balance. For stable drop shapes at infinite Λ, this high tangential stress limit forces the tangential flux to zero, so the surface is stagnated for any steady drop shape. For deforming interfaces, the tangential flux cannot be zero, but must balance local stretching to keep Γ nearly uniform.

Since Γ is nearly uniform, the interface dilutes as the drop stretches, causing the mean surface tension to increase and reducing the deformations relative to the clean interface case. However, the deformation cannot be predicted simply by setting the Marangoni stresses to zero and updating the surface tension with the diluted surface concentration at each timestep. Such a simulation was performed for $x = 0.996$; the resulting deformation curve is presented in figure 3(b), marked D. This curve predicts deformations that are lower than those realized from the full simulation.

The reason for the poor agreement is that the simple dilution simulation neglects the strong Marangoni stresses (see figure 5b). This stress is generated by a reduced surface tension at the drop pole relative to the value at the equator. The interface deforms more than the pure dilution case because of the weak tip stretching induced by this surface tension profile.

This is apparent in figure 5(c), where $\gamma(s)$ is shown for increasing x values. As the

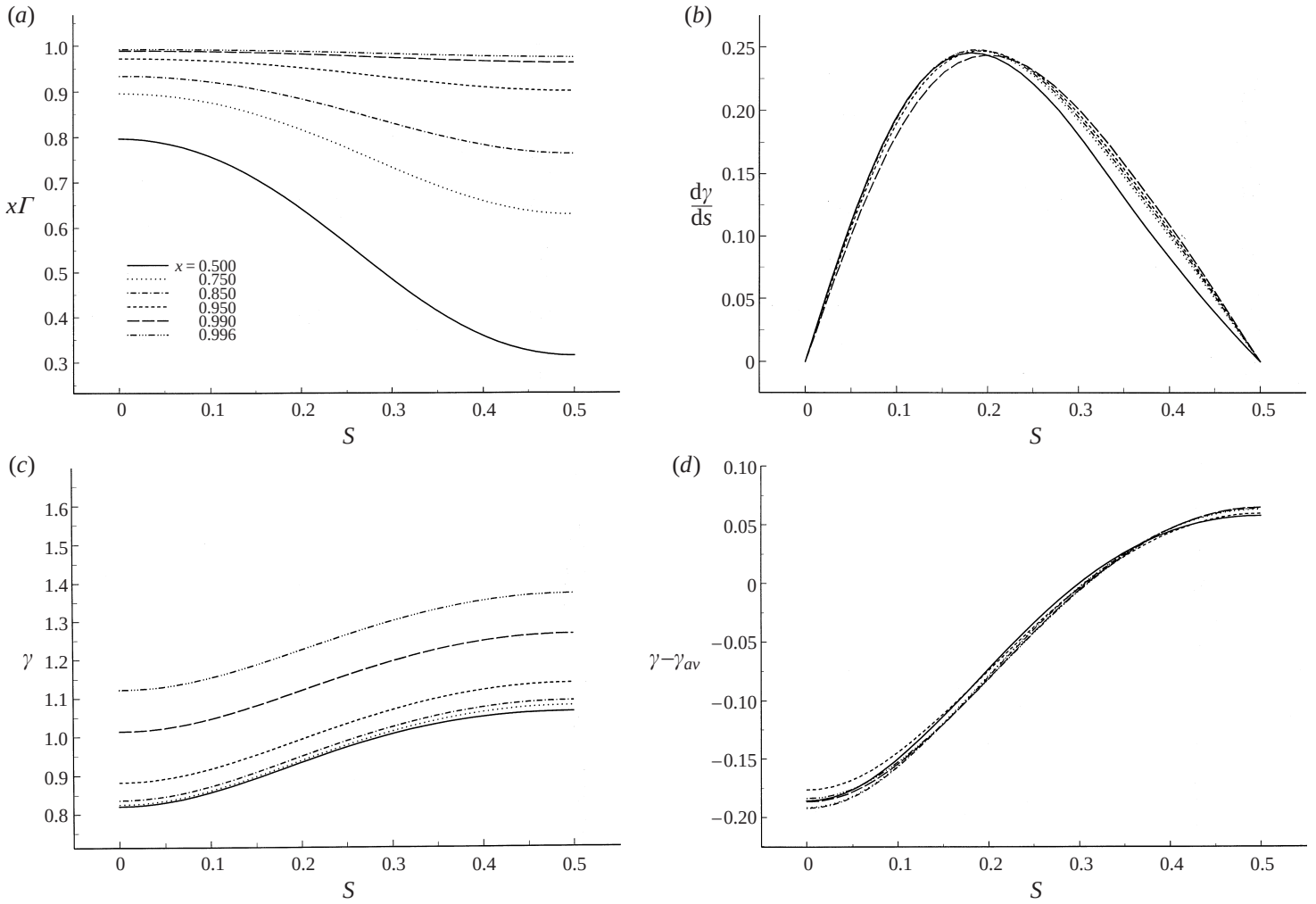

FIGURE 5. Families of curves as a function of x for $0.5 \leqslant x \leqslant 0.996$ for $Ca = 0.03$. The legend for all of figure 5 is an inset to figure 5(*a*). (*a*) $x\Gamma$ *vs. s* profiles. (*b*) Marangoni stress *vs. s* profiles. (*c*) γ *vs. s*; (*d*) $\gamma(s) - \gamma_{\mathrm{av}}$ *vs. s*.

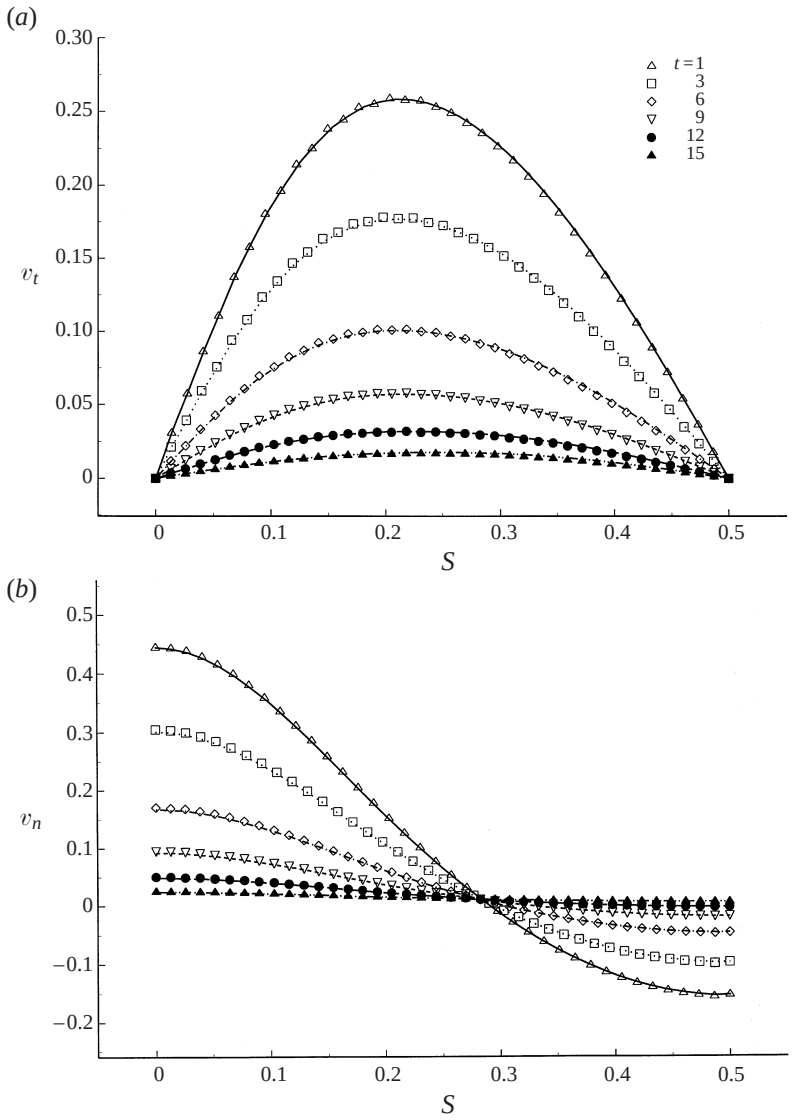

FIGURE 6. A comparison of the full (lines) and approximate (symbols) solutions for $x = 0.996$ for (*a*) v_t *vs.* s and (*b*) v_n *vs.* s as a function of time.

surface coverage increases, the surface tension profiles have nearly identical shape, but are displaced vertically. This shift in the dimensionless surface tension profiles is caused by the increased sensitivity of γ to dilution as x approaches 1. Plotting the surface tension as $\gamma(s) - \gamma_{av}$, where γ_{av} is based on the average surface concentration.

$$\Gamma_{av} = \frac{\int_{s=0}^{l} \Gamma \, \mathrm{d}s}{l}, \tag{24}$$

accounts for this dilution. The similarity of form is apparent, then, as these profiles can be superposed (see figure 5*d*).

These observations are used to simplify the surface mass balance in the limit of

x approaching unity. If the fluxes associated with the spatial variation of Γ are neglected, (20) becomes:

$$-\frac{1}{\Gamma}\frac{\partial \Gamma}{\partial t} = \frac{v_t}{r}\frac{\mathrm{d}r}{\mathrm{d}s} + \frac{\mathrm{d}v_t}{\mathrm{d}s} + 2H\, v_n = \nabla_s \cdot \boldsymbol{v}_s. \tag{25}$$

This mass balance governs the distribution of surfactant on a uniformly diluting interface. Noting that the (dimensional) surface concentration $\Gamma = N/A$, where N is the initial number of moles of surfactant on the interface, and A is the total area, this balance requires that the fractional global dilatation of the interface be equal to the local dilatation. The time evolution of v_t and v_n for both the full solutions and simulations are shown in figure 6(a) and 6(b). During the evolution of the drop shape, (25) does not constrain the interface to behave as if it were incompressible. (In fact, if the interface were incompressible, the drop shape would not change from its initial spherical geometry.) Rather, so long as the interface stretches to dilute Γ, the surface divergence of the velocity is non-zero. At steady state, the interface is incompressible; but since v_n is zero, v_t is also zero, so the interface is stagnant.

While (25) neglects the fluxes associated with spatial variations in Γ, it captures the dependence of Γ on arclength extremely well in the high coverage limit. In figure 7, the profiles from using either the simplified balance (25) or the full mass balance, (20) are compared for $x = 0.996$ as a function of Ca. The agreement is very good for Ca up to 0.05, for which the deformation is 0.15 (i.e. the drop length is nearly 35% longer than the breadth). For $Ca = 0.06$, the interface becomes increasingly dilute, i.e. $x\Gamma_{av} \sim 0.94$, less than the initial value of 0.996. As $x\Gamma$ reduces because of this dilution, the Marangoni stresses become less pronounced for a given Γ gradient. Gradients in Γ up to 10% over the length of the drop develop, so fluxes associated with gradients in Γ are no longer completely negligible. Still, the main features of the system are captured. The deformations superpose with the full simulation on the scale of the figure and agree to less than 1% at the highest Ca studied, with error decreasing as Ca is reduced. Similar agreement for all profiles was found for the transient results.

These results are observations from the numerical simulations; a strict perturbation analysis about x of unity was not performed because of the singularities in the normal and tangential stresses. As x approaches 1, not only do the tangential stresses diverge, but the surface tension strongly decreases. However, the pole in the tangential stress manifests first, as it is first order, and diverges faster than the logarithmic singularity in the normal stress balance. Because of this, the surface concentration is forced to be uniform by the tangential stresses at an x value for which the surface tension has not yet been strongly reduced. This is true in general for any surface equation of state that accounts for excluded area. For example, the two-dimensional van der Waals equation of state (see Davies & Rideal 1961), which has a first-order pole as x approaches unity in the surface tension and a second-order pole in its derivative. Again, the tangential stresses would diverge first, forcing Γ to be uniform, while the surface tensions are still finite.

In summary, for high surface concentration, the surface mass balance for the uniformly diluting interface requires that the tangential convective flux balances local surface dilatation. The tangential stresses that develop regulate the surface velocity so that this purely diluting interface condition is upheld. The normal stress balance is simply given by the integral of the tangential stress condition with respect to the arclength.

The limiting behaviour occurs because of the occurrence of a pole in the tangential

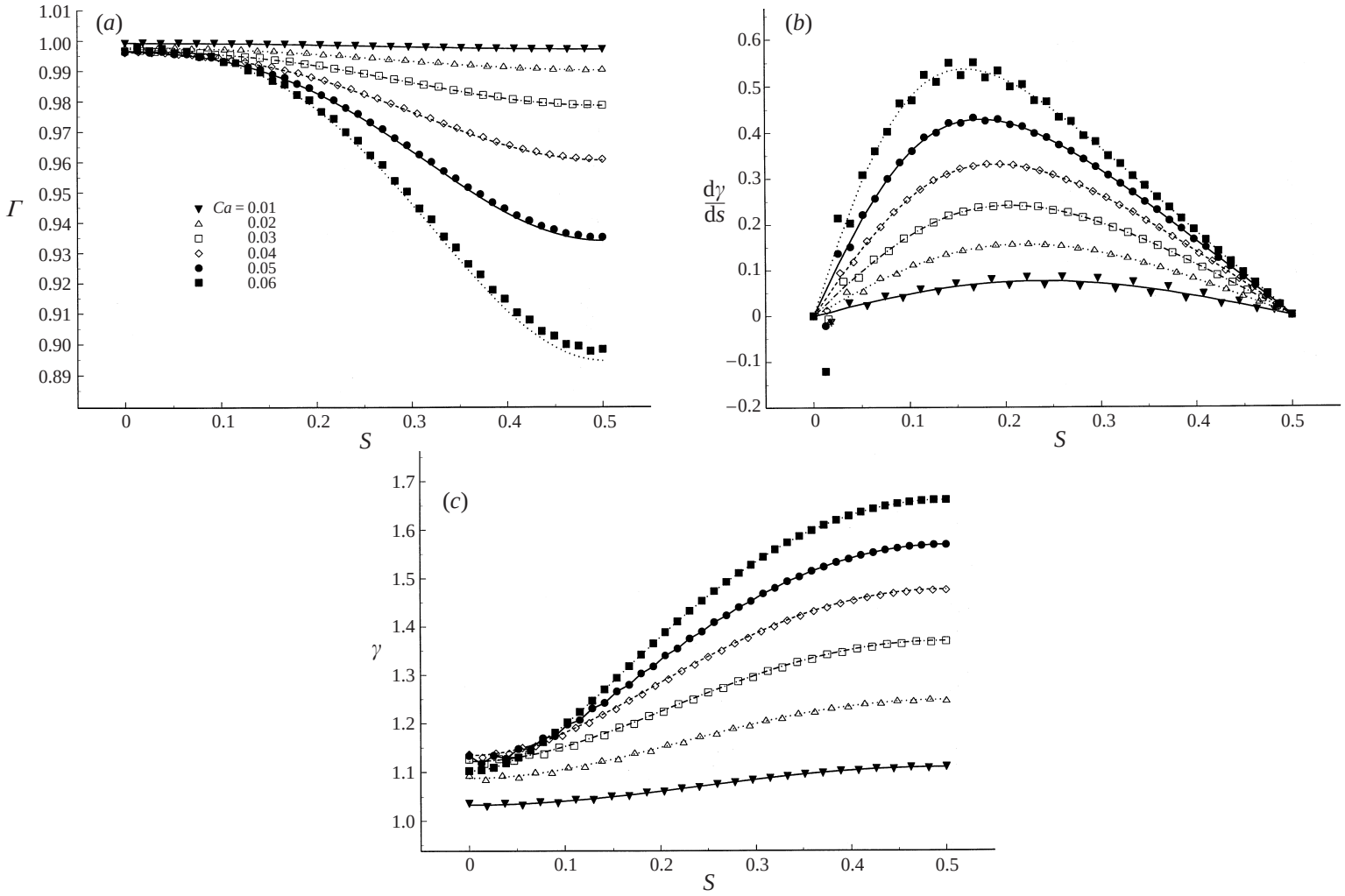

FIGURE 7. A comparison of the full (lines) and approximate (symbols) steady state solutions for $x = 0.996$ as a function of Ca. (*a*) Γ *vs. s* profiles. (*b*) Marangoni stress *vs. s* profiles. (*c*) γ *vs. s*. The deformations superpose with the full solution results.

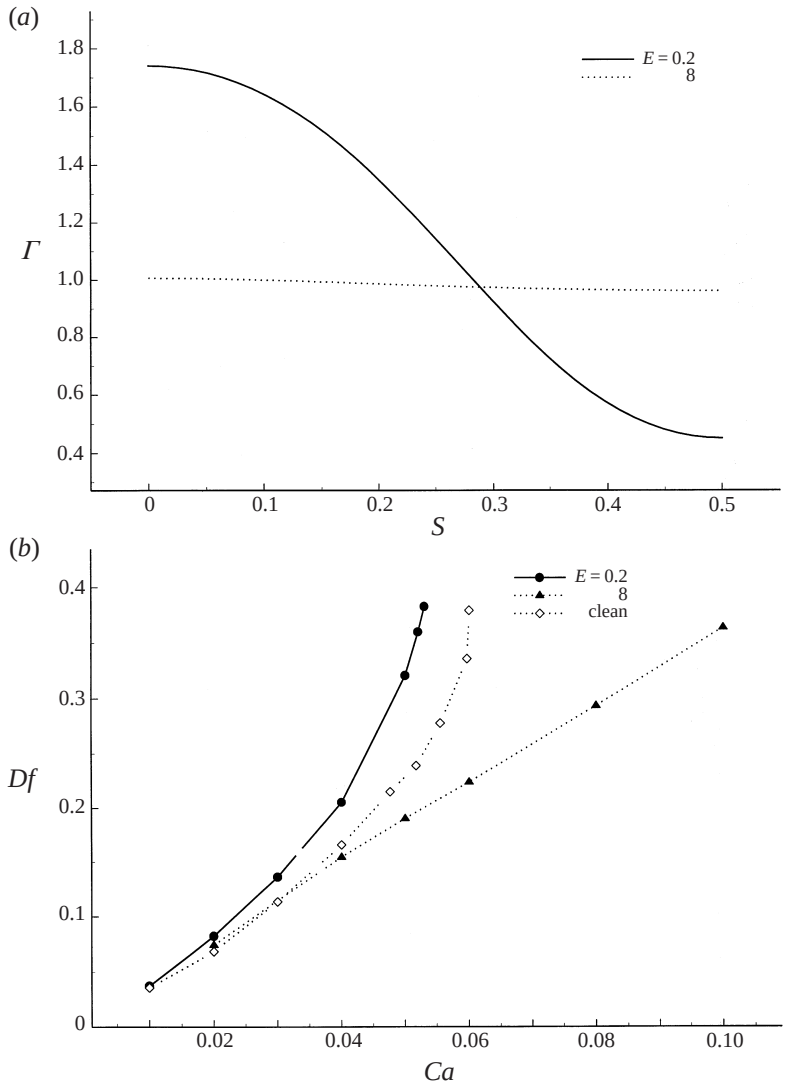

FIGURE 8. A comparison of profiles for $x = 0.5$ at $E = 0.2$ and $E = 8$, (*a*) Γ *vs. s* at $Ca = 0.04$; (*b*) Df *vs.* Ca.

stress of higher order than the pole in the normal stress. Considering the stress balance in the form:

$$\boldsymbol{n}\left[\left[-\frac{P}{Ca}\right]\right] + [[\boldsymbol{n}\cdot\boldsymbol{T}]] = -\frac{E}{Ca}\frac{x}{1-x\Gamma}\nabla_s\Gamma + \frac{1}{Ca}\left[\frac{\gamma_o}{\gamma_{eq}} + E\ln(1-x\Gamma)\right]2H\boldsymbol{n}, \quad (26)$$

it is clear that the tangential stress also requires uniform surface concentrations for either infinite E or small Ca. However, neither limit is interesting physically. For finite E and infinitesimally small Ca, the surface does not deform. The tangential stresses demand that Γ remain uniform; the mass balance requires that v_t be zero. Therefore, this limit corresponds to a non-deforming stagnant particle. In the limit of infinite E, finite Ca, the surface tension reduces without bound, and the interface becomes undefined.

The surface saturation behaviour observed in this study occurs at finite values of E/Ca. The larger this ratio is, the smaller the x value for which Γ remains uniform because of strong Marangoni stresses. For example, in figure 8(a) and 8(b), the Γ and Df profiles are compared at $x = 0.5$ for $E = 0.2$ and $E = 8.0$ at fixed Ca. The Γ profile for the higher E value has significantly weaker gradients; the deformation Df remains dilution dominated throughout the deformation process. Thus, overestimating the coupling between γ and Γ prevents the low-concentration behaviour of the interface from being captured.

The impact of surface saturation on the stagnant cap formation for spherical droplets was studied by He *et al.* (1991). Their results indicate that for fixed E values, the cap angle is greater for the model adopted here than for the linear equation of state. This is simply because the linear equation does not obey saturation, and therefore allows surfactant to be packed more strongly at the pole. This strongly underestimates the degree of stagnation of the interface. Here the surface is shown to be completely stagnated for surface coverages as low as 0.5 for $E = 0.2$. The linear equation of state would give the Marangoni stress dependence as :

$$[[\boldsymbol{n} \cdot \boldsymbol{T} \cdot \boldsymbol{t}]] = -E \frac{x}{Ca} \frac{\partial \Gamma}{\partial s}. \tag{27}$$

A completely stagnated surface might be realized for the drop in the extensional flow for the linear constitutive behaviour, but only if unrealistically large values for E are adopted. Note, however, that the linear model has potential complications since the surface tension tends to zero as rapidly as the tangential stress diverges.

The volume average stress tensor is calculated to understand the rheology of dilute dispersions (Taylor 1932). The particle contribution to this stress is given by Σ:

$$\Sigma = \int_S (2H\gamma \boldsymbol{n} + \nabla_s \gamma)\boldsymbol{x} \, \mathrm{d}A, \tag{28}$$

where S is the surface of the drop. The two components of Σ are shown in figure 9 as a function of x and Ca. When scaled with the clean interface surface tension, γ_o/a, both Σ_{rr} and Σ_{zz} decrease monotonically as x increases because the equilibrium surface tension decreases (see figure 9(a)(ii) and 9(b)(ii)).

When scaled with γ_{eq}/a, however, Σ_{zz} increases monotonically with x and Ca, as expected, since the Marangoni stresses which oppose $\boldsymbol{v}_s$ (which has a strong axial component) also obey this trend. The radial component Σ_{rr} varies non-monotonically with x. At fixed Ca, the greater the deformation Df, the smaller the cross-section of the droplet, and the smaller is Σ_{rr}. The variation of Σ_{rr} with Ca also depends on x. For $x < 0.85$, Df is larger than the clean case, and increases strongly with Ca. Thus, the cross-section of the drop diminishes, and Σ_{rr} decreases with Ca. For x of 0.95 or greater, however, Df is less than the clean interface case and decreases weakly with Ca. The weak changes in cross-section do not determine Σ_{rr}; rather, the large Marangoni stresses in this regime cause Σ_{rr} to increase with Ca.

4. Conclusions

An upper bound exists on the surface concentration that can be adsorbed in a monolayer because of the finite dimensions of surfactant molecules. In this study, the behaviour of a droplet in an extensional flow is studied for physically relevant values of the surfactant material parameters. The hydrodynamics are strongly

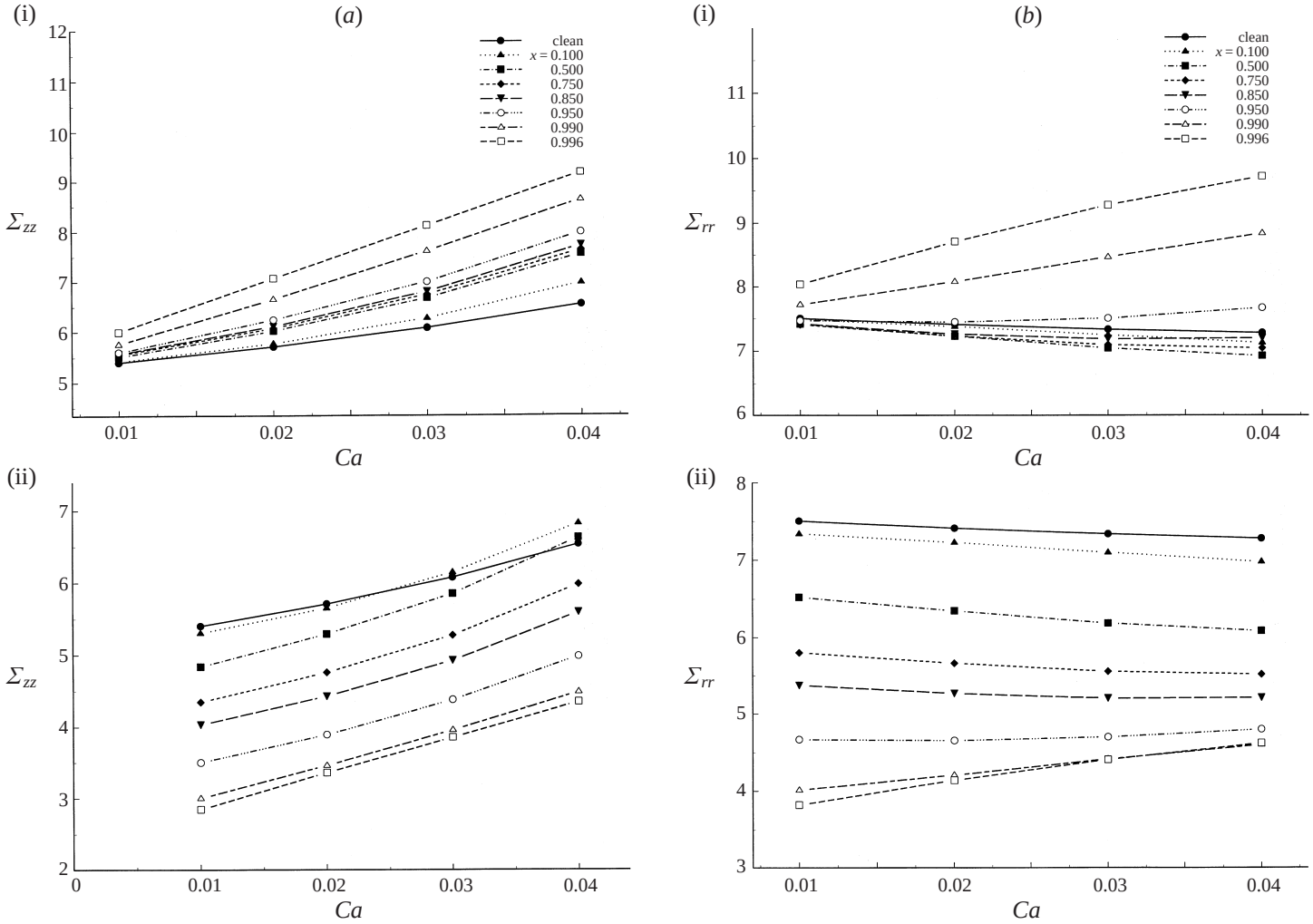

FIGURE 9. The particle contribution to the volume averaged stress tensor (*a*) (i) Σ_{zz} (scaled with γ_{eq}/a) as a function of x and Ca. (ii) Σ_{zz} scaled with γ_o/a. (*b*) (i) Σ_{rr} (scaled with γ_{eq}/a) as a function of x and Ca. (ii) Σ_{rr} scaled with γ_o/a.

altered by varying the fraction of the interface initially covered by insoluble surfactant.

Stagnant tips form on the droplet once steady shapes are attained at low surface coverage ($x \ll 1$). The stagnation spans from the tips to some arclength. From this arclength to the equator, the interface is mobile. The portion of the interface stagnated increases with x, unitil the entire interface is completely stagnant.

A full range of deformation behaviours are realized with increasing x, from strong tip stretching with concomitant strong Γ gradients at low x to dilution dominated deformations with weak Γ gradients at larger x.

The effect of surface saturation for an insoluble surfactant is to generate large Marangoni stresses for perturbative departures of the surface concentration from a uniform distribution. This observation is exploited to simplify the surface mass balance by assuming that fluxes associated with surface concentration gradients are negligible. The results from this simplified formulation are shown to agree with the full simulation.

This simplified mass balance is an extension of the stagnant surface limit commonly invoked for non-deforming surfactant-laden interfaces, and reduces to a stagnated surface condition at steady state. This framework should simplify the study of pronounced Marangoni effects at high surface concentration on deforming interfaces.

Stagnant tip formation may be important in the phenomenon of tip streaming, in which small droplets are shed from the pointed parent drop tips (deBruijn 1993). Tip streaming has been observed either in fluids of unknown purity or for low surfactant concentrations on drops of viscosity ratio less than unity. As the surfactant concentration is increased, tip steaming is suppressed. In the experiments of deBruijn, tip streaming on drops in shear flows was investigated. The surface tension of the small droplets that were shed was far lower than that of the parent drops, suggesting that surfactant has accumulated at the tips of the parent drop.

The mechanisms described in this paper provide a potential explanation for these observations. At dilute surfactant concentration, stagnant tips form, with significant accumulation of surfactant in the tip regions. This promotes increases in local curvature. For low-viscosity fluids, this may lead to pointed tips like those observed in experiment. For Ca large enough to promote drop shedding, drops shed from these tips would be rich in surfactant, with surface tensions lower than the parent drops. At elevated concentration, the coverage x increases, suppressing the occurrence of large surface concentration gradients. Or, if adsorption/desorption exchange is rapid, the effect of increasing bulk concentration is to decrease the effective bulk diffusion timescales, allowing the surfaces to be restored to a uniform surface concentration and a stress-free interface. In either case, the accumulation of surfactant at the tips that form at low concentration would be eliminated.

Finally, these results underscore that a nearly uniform surface concentration profile does not imply that an interface is remobilized (or behaving hydrodynamically as if it were clean). Remobilization occurs only if the surfactant mass transfer is rapid enough to keep the surface concentration uniform and in equilibrium with the surrounding solution (Stebe, Lin & Maldarelli 1991; Wang, Maldarelli & Papageorgiou 1999). In the absence of mass transfer between the interface and the bulk, however, only Marangoni stresses and surface diffusion act to enforce the maximum packing limit. Typically, surface diffusion is weak. Thus, as demonstrated in this study, strong Marangoni stresses resist the local accumulation of surfactant, forcing the surface concentrations to be uniform in this limit.

REFERENCES

Chang, C. H. & Franses, E. 1995 Adsorption dynamics of surfactants at the air–water interface: a critical review of mathematical models, data and mechanisms. *Colloids and Surfaces* A **100**, 1.

Davies, J. T. & Rideal, E. K. 1961 *Interfacial Phenomena*. Academic Press.

Davis, R. E. & Acrivos, A. 1966 The influence of surfactants on the creeping motion of bubbles. *Chem. Engng Sci.* **21**, 681.

deBruijn, R. A. 1993 Tip streaming of drops in simple shear flows. *Chem. Engng Sci.* **48**, 277.

Defay, R. & Prigogine, I. 1966 *Surface Tension and Adsorption*. John Wiley.

Edwards, D., Brenner, H. & Wasan, D. 1991 *Interfacial Transport Processes and Rheology*. Butterworth-Heinemann.

Eggleton, C. D. & Stebe, K. J. 1998 An adsorption-desorption controlled surfactant on a deforming droplet *J. Colloid Interface Sci.* **208**, 68.

Frumkin, A. 1925 Die Kapillarkurve der hoheren Fettsauren und die Zustandsgleichung. **116**, 466.

Guggenheim, E. A. 1952 *Mixtures*. Oxford University Press.

He, Z., Maldarelli, C. & Dagan, Z. 1991 The size of stagnant caps of bulk soluble surfactants on interfaces of translating fluid droplets. *J. Colloid Interface Sci.* **146**, 442.

Ladyzhenskaya, O. A. 1969 *The Mathematical Theory of Viscous Incompressible Flow*. Gordon and Breach.

Levich, V. G. 1962 *Physicochemical Hydrodynamics*. Prentice-Hall.

Lin, S. Y., Tsay, R., Lin, L. & Chen, S. 1996 Adsorption kinetics of $C_{12}E_8$ at the air–water interface: adsorption on a clean interface. *Langmuir* **12**, 6530.

Milliken, W. J. & Leal, L. G. 1994 The influence of surfactant on the deformation and breakup of a viscous drop: the effect of surfactant solubility. *J. Colloid Interface Sci.* **166**, 275.

Milliken, W. J., Stone, H. A. & Leal, L. G. 1993 The effect of surfactant on the transient motion of Newtonian drops. *Phys. Fluids* A **5**, 69.

Pan, R., Green, J. & Maldarelli, C. 1998 Conditions for promoting kinetic influence during surfactant exchange at an interface and their use for measuring kinetics parameters by the pendant bubble method. *J. Colloid Interface Sci.* **205**, 213.

Pawar, Y. P. & Stebe, K. J. 1996 Marangoni effects on drop deformation in an extensional flow: the role of surfactant physicochemistry. I. Insoluble surfactants. *Phys. Fluids* **8**, 1738.

Pozrikidis, C. 1992 *Boundary Integral and Singularity Methods for Linearized Viscous Flows*. Cambridge University Press.

Rallison, J. M. 1984 The deformation of small viscous drops and bubbles in shear flows. *Ann. Rev. Fluid Mech.* **16**, 45.

Sadhal, S. S. & Johnson, R. E. 1983 Stokes flow past bubbles and drops partially coated with thin films. Part 1. Stagment cap of surfactant films: Exact solution. *J. Fluid Mech.* **126**, 237.

Stebe, K. J., Lin, S. Y. & Maldarelli, C. 1991 Remobilizing surfactant retarded fluid particle interfaces. I. Stress-free conditions at the interfaces of micellar solutions of surfactants with fast sorption kinetics. *Phys. Fluids* **3**, 3.

Stone, H. A. 1990 A simple derivation of the time-dependent convective-diffusion equation for surfactant transport along a deforming interface. *Phys. Fluids* A **2**, 111.

Stone H. A. 1994 Dynamics of drop deformation and breakup in viscous fluids. *Ann. Rev. Fluid Mech.* **26**, 65.

Stone H. A. & Leal, L. G. 1990 The effects of surfactants on drop deformation and breakup. *J. Fluid Mech.* **220**, 161.

Taylor, G. I. 1932 The viscosity of a fluid containing small drops of another fluid. *Proc. R. Soc. Lond.* A **138**, 41.

Wang, Y., Maldarelli, C. & Papageorgiou, D. 1999 Increased mobility of a surfactant retarded bubble at high bulk concentrations. *J. Fluid Mech.* in press.

Watkins, J. C. 1968 The surface properties of pure phospholipids in relation to those of lung extracts. *Biochim. Biophys. Acta* **152**, 293.

Wong, H., Rumschitzski, D. & Maldarelli, C. 1996 On the surfactant mass balance at a deforming fluid interface. *Phys. Fluids* **8**, 3203.